Textile-Based Batteryless Moisture Sensor

Xiaochen Chen, Han He, Zahangir Khan, Lauri Sydänheimo, Leena Ukkonen, Johanna Virkki

***Abstract*—In this paper, we established a new type of passive Ultra-High-Frequency (UHF) Radio Frequency Identification (RFID) technology-based sensor with a referenced readout for moisture. We introduced the sensor system, which consisted of a sensor tag and a reference tag. In a highly moist environment, the sensor tag, which was fabricated by embroidery and 3D printing, permanently changed its shape from flat to curved, which then influenced its wireless performance. By recording the backscattered powers of the sensor tag and the unaffected reference tag, the presence of moisture could be detected. Based on our preliminary results, when the mean value of ΔP% was higher than 80%, the sensor system indicated exposure to high moisture environment. Our moisture sensing system can provide cost-effective zero-energy monitoring of moisture exposure for versatile application fields.**

***Index Terms*—passive UHF RFID technology, moisture sensor, wireless sensor, 3D printing, embroidery, zero-energy.**

I. Introduction

RADIO Frequency Identification (RFID) is nowadays a well-assessed technology for tracking and tracing procedures [1][2]. Also more complex applications are being researched worldwide, concerning for example sensing [3]-[7], localization [8], wearable devices [9]-[11], and also more-efficient supply chains [12][13]. Further, intelligent packaging technologies [14] and equipment of traditional packages with intelligence (to sense the product's condition or the ambient conditions) have been studied [15][16]. Due to the wireless, battery-less, and thus maintenance-free nature, especially passive RFID-based sensors have attracted a growing interest [17]-[20]. With the help of self-sensing materials, RFID tags will have detectable changes of wireless performance, caused by a specific environmental condition. This feature can be utilized in several types of passive UHF RFID sensor antenna systems [21]-[23]. These self-sensing components have the benefits of low-cost, simple fabrication, and eco-friendliness. The sensing systems can be used as the part of the Internet-of-Things (IoT) [24] for example for monitoring health information through human's skin [25]-[27], detecting noxious gases in underground mines [28]-[30], or sensing the temperature levels of the environment [31].

In addition, as has been shown in case of strain and compression sensing, involving a reference tag in the sensor system will greatly help to increase the accuracy of the sensing system in practical use [32][33]. Also our goal is to move away from fixed RFID reader-RFID sensor tag systems and present sensor tags with a reference readout.

In this paper, we present a cost-effective passive RFID moisture sensing system for the global UHF RFID frequency band, fabricated by embroidery and 3D printing technology. This new type of sensor system consisted of a flexible sensor tag (which will curve automatically and permanently after dipped into water) and a stable reference tag. As studied in [35], curving of an RFID dipole antenna significantly changes the wireless performance of the tag. Thus, in our approach it can be utilized to detect moisture. Such a low-cost solution will be useful for example in detecting moisture exposures in various supply chains and in transportation mishandling of moisture sensitive items, as well as in indicating ice melting during frozen transportation.

II. Antenna Design and Simulation

The wire in the antenna body of the sensor tag had the same width (1.2 mm) in all parts of the antenna. The identical antenna structure used for the sensor tag and the reference tag is shown in Fig. 1.

In this sensor system, the wireless response of the sensor tag was used to detect the presence of environmental moisture, while the wireless performance of the reference tag remains stable. The backscattered signals of passive RFID tags are noisy and unstable, and strongly affected by the environment. By involving the reference tag, the influence of the environment can be minimized.

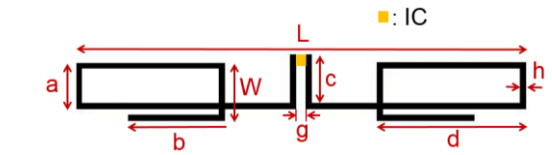

L	W	a	b	c	d	h	g
121.8	15.4	12.2	20.5	14.4	40.1	1.2	3

Fig. 1. Structure and size of the sensor tag, unit in mm.

Firstly, the sensor antenna was designed and optimized to be functional throughout the global UHF RFID frequency band, which will support its use in global supply chain management. The antenna body material was conductive thread and the sheet resistance of the antenna material was simulated as 0.2 ohm/square. In the simulation, the substrate consists of two

This research was funded by the Academy of Finland and Jane and Aatos Erkko Foundation.

All authors are with the Faculty of Medicine and Health Technology, Tampere University, Tampere 33720, Finland (e-mail: xiaochen.chen@tuni.fi; han.he@tuni.fi; zahangir.khan@tuni.fi; lauri.sydanheimo@tuni.fi; leena.ukonen@tuni.fi; johanna.virkki@tuni.fi)

parts: 0.5 mm polyamide (relative permittivity 4.3 and loss tangent 0.004 in HFSS preset) and 1.5 mm of 3D-printed material (relative permittivity 3.51 and loss tangent 0.03 at the original condition and relative permittivity 3.5 and loss tangent 0.0413 when exposed to moisture, measured by a vector network analyzer, as presented in [23]). The antenna was first located on a surface of a 130 mm × 40 mm flat substrate (to simulate dry condition), as shown in Fig. 2.

To simulate the curved senor tag, the flat substrate was changed into a semicircle with a radius of around 40 mm (as the perimeter of the round was double substrate length, 130 mm × 2 = 260 mm) and radian π, as shown in Fig. 3. The antenna was still on the surface of the substrate. The simulated realized gain of the antenna in both flat and curved structure is shown in Fig. 4, where the H-plane and E-plane realized gains are shown at 915 MHz. In the E-plane, the realized gain of the curved antenna increased at ±90° obviously and shrinked slightly at 0° and 180°. It was caused by the RFID dipole antenna structure curving, as studied in [35].

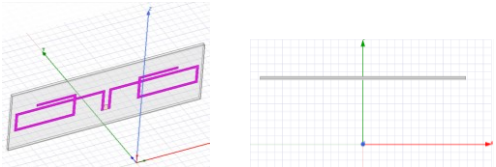

Fig. 2. Flat simulation: overall view (left) and top view (right).

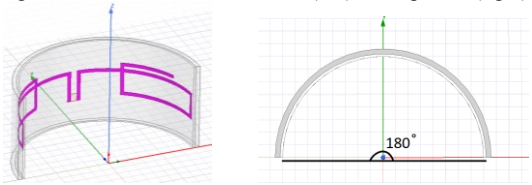

Fig. 3. Curved simulation: overall view (left) and top view (right).

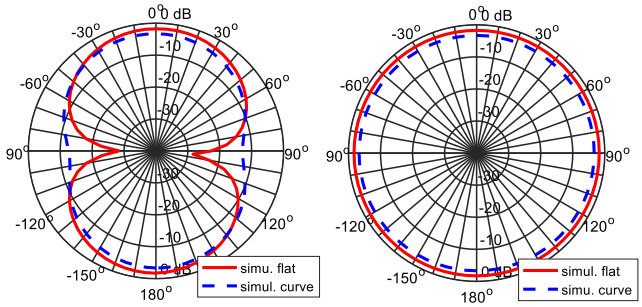

Fig. 4. Realized gain in simulation of the flat antenna and curved antenna in E-plane (left) and H-plane (right).

III. Fabrication

The sensor tag antenna body was fabricated from conductive thread. It was embroidered on a plain knitting elastic band, using Husqvarna Viking sewing machine. The used thread was multifilament silver plated thread (Shieldex multifilament thread 110f34 dtex 2-ply HC). The DC linear resistivity of the thread is 500±100 Ω/m, and the diameter is approximately 0.16 mm. The elastic band was strained to 127 % of its original length before the embroidery process to achieve the functionality, i.e., curving of the sensor. The ready-made embroidered tag antenna on elastic band is shown in Fig. 5. The reference tag was fabricated in an identical way, but the elastic band was not initially strained. Thus, in this case, the elastic band did not try to return to its initial shape when the 3D-printed layer on top of it got soft. Consequently, the reference tag stayed flat even when exposed to moisture.

After antennas fabrication, NXP UCODE G2iL series RFID ICs, provided by the manufacturer in a strap with copper pads, as shown in Fig. 5, were attached to the antennas. The IC was located on the designed position directly without conductive glue or embroidery connection. The added 3D-printed layer on top of the antenna will press the IC on the antenna to create and hold the needed connection.

Next, a 3D-printed Poro-lay gel-lay porous filament substrate layer was applied on the top of the embroidered antenna and IC by Prenta Duo XL 3D printer, as shown in Fig. 6 (A, top view), (B, bottom view) and (C, side view). The size of the printed layer was 130 mm × 40 mm and the used printing parameters are shown in Table 1. This 3D-printed material is made from a rubber-elastomeric polymer and a polyvinyl alcohol (PVA)-component. When in water, the PVA component disappears and the rubber polymer remains, which means the printed pattern will become flexible in water.

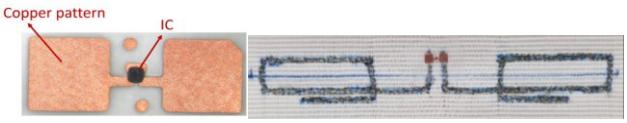

Fig. 5. The used IC structure (left) and a readymade sensor tag (right).

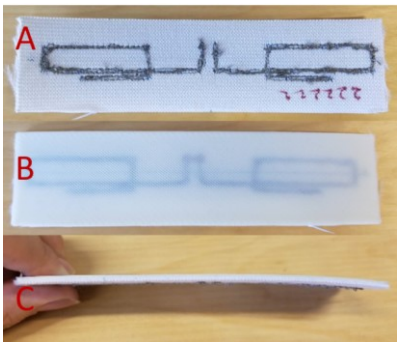

Fig. 6. Ready-made sensor A) front B) back C) side.

Table. 1. Substrate printing parameters

3D printing parameters	
Printing head temperature	220 °C
Plate temperature	50 °C
Infill percentage	60 %
Thickness	1.5 mm
Infill Pattern	Rectilinear

IV. Wireless Measurements

A. *Sensor functionality testing*

To test the sensor functionality, the system was dipped into water for one hour, until the PVA component of the 3D-printed structure was totally dissolved. Then, the 3D-printed structure became soft and the sensor tag got curvy as shown in Fig. 7, while the reference tag stayed flat. The 3D-printed layer started getting softer immediately when in water, as it had a slight curve already after 5 minutes. The curvatures of the tag after different soaking times are shown in Fig. 7. In this study, the 3D-printed substrate stayed in water for 1 hour, after which it

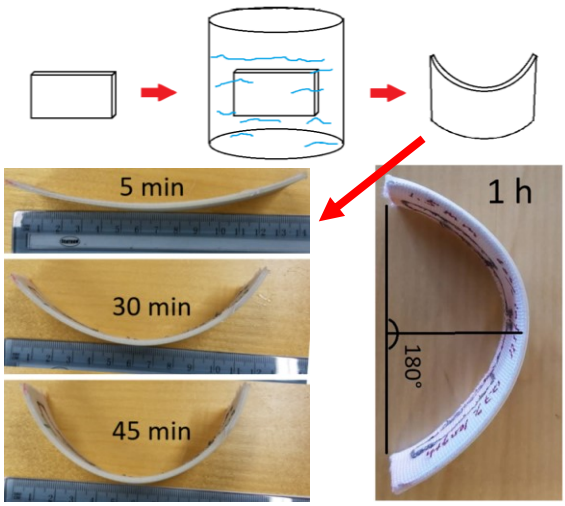

Fig. 7. The sensing process of the sensor tag.

was totally soft and the final shape appeared. When the sensor structure was dry again, it was hardens as it was prior to dissolving, but maintained its curvy shape.

The moisture sensor tags were tested in an anechoic chamber firstly, to compare their radiation patterns to simulated ones. The sensor tags were measured using a measurement system (Voyantic Tagformance) containing an RFID reader unit with a capability to a power-frequency sweeps. All the measurements were conducted with the tag suspended on a foam fixture in the anechoic chamber.

During the test, we recorded the lowest continuous-wave transmission power (threshold power: P_{th}) at which a valid 16-bit random number from the tag is received as a response to the query command in ISO 18000-6C communication standard. In addition, the wireless channel from the reader antenna to the location of the tag under test was first characterized using a system reference tag with known properties. As has been detailed in [6], this enabled us to estimate the attainable read range of the tag (d_{tag}) versus frequency from:

$$d_{tag} = \frac{\lambda}{4\pi}\sqrt{\frac{EIRP}{\Lambda}\frac{P_{th^*}}{P_{th}}}, \quad (1)$$

where λ is the wavelength transmitted from the reader antenna, P_{th} is the measured threshold power of the tag, Λ is a known constant describing the sensitivity of the system reference tag, P_{th^*} is the measured threshold power of the system reference tag, and *EIRP* is the emission limit of an RFID reader, given as equivalent isotropic radiated power. We present all the results corresponding to *EIRP* = 3.28 W, which is the emission limit in European countries.

The realized gains of the tags were analyzed using the path-loss measurement data from the measurement unit. The realized gain (G_r) takes into account the antenna–IC impedance matching and can be calculated as:

$$G_r = \frac{P_{IC,TS}}{L_{fwd} \times P_{th}} \quad (2)$$

where $P_{IC,TS}$ is the tag IC sensitivity, L_{fwd} is the measured forward losses.

The calculated read ranges of the sensor tag and the reference tag are shown in Fig. 8. The read ranges of the sensor tag (at the

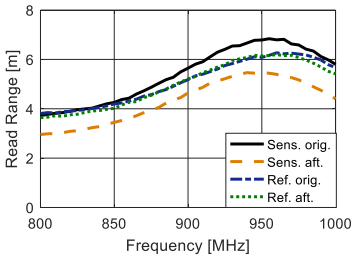

Fig. 8. Read ranges of the sensor tag and the reference tag before and after dipped into water.

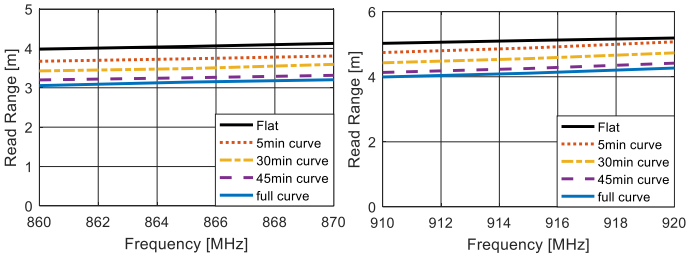

Fig. 9. Read range of the sensor tag versus the time in water in the European UHF RFID frequency band (left) and US frequency band (right).

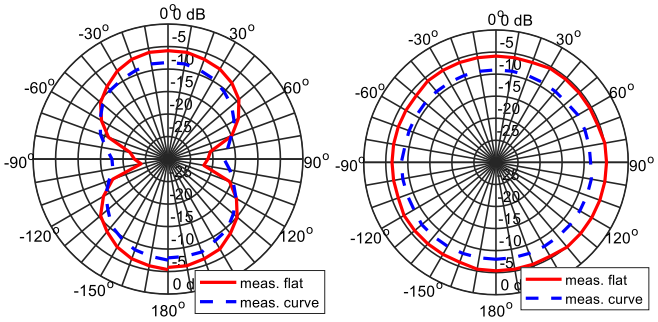

Fig. 10. Radiation patterns in measurements of the flat antenna and curved antenna in E-plane (left) and H-plane (right).

European and US UHF RFID frequencies) versus the time in water are shown in Fig. 9. The read range was initially around 4-6 meters between 866 MHz to 915 MHz frequency bands, which cover both European and the US RFID standard frequency bands. Thus, this moisture sensor system can be used globally. The radian of the sensor increased with the socking time while the read range decreased. After dipped into water for 1 hour, the tag curves to form a half-round. The measured curved read range result, which was around 3-5 meters between 866 MHz to 915 MHz, was slightly shorter than in the initial flat condition. This decreasing was caused by the impedance changing mainly due to antenna curving [35]. The antenna gain has changed as well with the deformation, as shown in the plot of the radiation pattern (Fig. 10). This shows that the change in the antenna performance also slightly contributes to the change in the read range. The measured realized gain, as shown in Fig. 10, also increased at ±90° obviously and shrinked slightly at 0° and 180° in E-plane. However, they shrinked a little bit more, when compared to the simulated results at both E- and H-plane. One possible reason was that the normal embroidery machine can only fabricate the antenna with the accuracy of mm. Thus, the ready-made antenna may have little size differences from the design in the simulation.

For the reference tag, the read range remained same from 866

MHz to 915 MHz, after dipped into water and dried again. This supported the conclusion that the change of the sensor tag performance was caused by the structure transformation, not by the variation of the electrical properties of the non-conductive substrate. The minimum read ranges of the system were around 3 meters at the global UHF RFID frequencies. These read ranges can still meet the requirements of many of the discussed practical applications.

B. Practical sensor testing

In practical sensor testing, Thing Magic M6 RFID reader with a circular polarized reader antenna was used for recording the backscattered powers. As explained, in the sensing system, the reference tag was located near the sensor tag, since the signal from the reader to the closely spaced tags travels approximately through the same channel. As showed in Fig. 11, the reference tag was located orthogonally of the sensor tag with a 3 cm distance.

The tags were tested in two different office conditions, as shown in Fig. 12. The backscattered powers of both tags were measured at 1 meter from the reader and the transmitted power was 28 dBm at 866 MHz. The measured RSSI (received signal strength indicator) values of each tag are shown in Tables 2 and 3. The reference tags had a stable wireless performance with flat and curved sensor tag structures in both environments. As for the sensor tags, the backscattered power changed clearly between the flat and the curved stage, which was promising for practical use of these sensors.

In this study, we indicated the presence of water by calculating the variation of the backscattered power strength,

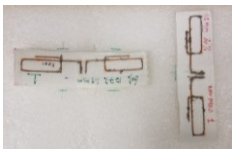

Fig. 11. Configuration of the sensor tag and reference tag.

Fig. 12. Practical measurement in office condition 1 (top) and corridor condition 2 (bottom)

Table 2. The backscattered power of flat sensor (Sens. f) and reference tag (Ref. f) as well as curved sensor (Sens. c) and reference tag (Ref. c) in environment 1, unit in dBm.

Counts	1	2	3	4	5	6	7	8	9	10
Sens. f	-34	-34	-34	-34	-33	-33	-34	-34	-34	-34
Ref. f	-33	-33	-33	-33	-33	-33	-33	-33	-33	-33
Sens. c	-44	-44	-44	-44	-43	-44	-43	-44	-44	-44
Ref. c	-34	-34	-34	-34	-35	-34	-35	-35	-35	-35

Table 3. The backscattered power of flat sensor (Sens. f) and reference tag (Ref. f) as well as curved sensor (Sens. c) and reference tag (Ref. c) in environment 2, unit in dBm

Counts	1	2	3	4	5	6	7	8	9	10
Sens. f	-40	-42	-40	-40	-42	-42	-42	-40	-42	-40
Ref. f	-40	-42	-40	-38	-42	-42	-42	-40	-40	-42
Sens. c	-32	-32	-32	-32	-32	-32	-32	-33	-32	-32
Ref. c	-37	-36	-37	-37	-36	-36	-36	-36	-36	-36

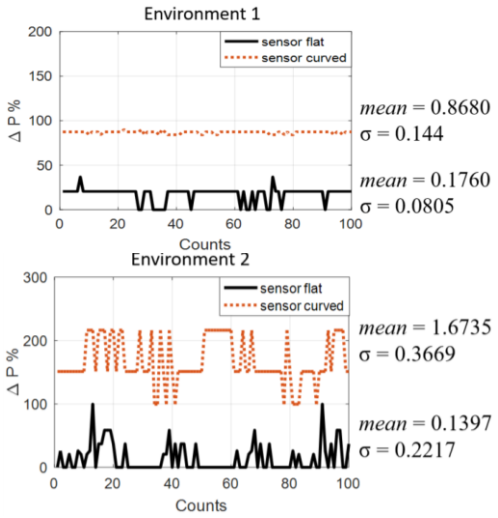

Fig. 13. Calculated $\Delta P\%$ of flat and curved sensor tag in environment 1 (top) and environment 2 (bottom).

defined as $\Delta P\ \% = \left|\frac{P_{sns}-P_{ref}}{P_{ref}}\right|$, where P_{sns} and P_{ref} were the backscattered power strength from the sensor tag and the reference tag, respectively. Fig. 13 shows the calculated *ΔP %* as well as the mean value and the standard deviation of the measurements in both environments. *ΔP%* was around 20% and 90% in the 100 read counts, when the sensor was flat and curved, respectively, in environment 1. In environment 2, *ΔP%* changed from around 10% to 170%, before and after the sensor got curved, respectively. Thus, by recording the backscattered power of the system and calculating *ΔP%,* the presence of moisture can be tracked. While the mean of *ΔP%* was less than 20%, the environment had stayed dry. When the mean of *ΔP%* was higher than 80%, it indicated exposure to moisture. These preliminary results show that this system can sense the exposure to moisture.

V. Conclusions

In this paper, we presented the design, fabrication, wireless evaluation, and practical testing of a wireless passive sensor system with a referenced readout for moisture. The sensor tag was fabricated by a combination of embroidery and 3D printing technology. This structure enabled the passive UHF RFID sensor tag to change shape permanently, after exposed to water for 1 hour. The measured estimate read range of all the tags were more than 3 to 5 meters, which were very promising for the practical applications. By measuring and comparing the change in the backscattered power percentage (*ΔP%)*, the presence of moisture could be detected and recorded. In practical environments, when the mean value of *ΔP%* was higher than 80%, the sensor system showed that it had been in a highly moist condition. This type of cost-effective and battery-free sensor system has versatile applications for example in supply chain monitoring. After these preliminary results, further testing will be done with a larger amount of samples. The next steps include testing the effects of water temperature on the sensor performance, as well as testing the sensor with other liquids.

REFERENCES

[1] Hopeland Technologies CO. Ltd., RFID in supply chain management, [Accessed on 02.10.2019], Available at: http://www.hopelandrfid.com/blog/rfid-in-supply-chain-management_b34.

[2] M. M. Honari, H. Saghlatoon, R. Mirzavand and P. Mousavi, "An RFID sensor for early expiry detection of packaged foods," 2018 18th International Symposium on Antenna Technology and Applied Electromagnetics (ANTEM), Waterloo, ON, 2018, pp. 1-2.

[3] C. Occhiuzzi, S. Caizzone and G. Marrocco, "Passive UHF RFID antennas for sensing applications: Principles, methods, and classifcations," in IEEE Antennas and Propagation Magazine, vol. 55, no. 6, pp. 14-34, Dec. 2013.

[4] X. Song, G. Wang and Y. He, "Design of the high-sensitivity RFID sensor tag with MOEA/D-DE," 2016 International Symposium on Antennas and Propagation (ISAP), Okinawa, 2016, pp. 950-951.

[5] T. Kaufmann, D. C. Ranasinghe, M. Zhou, C. Fumeaux, "Wearable quarter-wave folded microstrip antenna for passive UHF RFID applications," in International Journal of Antennas and Propagation, Article ID 129839, 2013

[6] O. O. Rakibet, C. V. Rumens, J. C. Batchelor, S. J. Holder, "Epidermal passive RFID strain sensor for assisted technologies," IEEE Antennas Wireless Propagation Letter, 13, 2014.

[7] C. Occhiuzzia, C. Vallese, S. Amendola, S. Manzari, G. "Marrocco, NIGHT-Care: A Passive RFID system for remote monitoring and control of overnight living environment," Procedia Computer Science, 32, 2014.

[8] Borda, RFID real-time tracking, [Accessed on 02.01.2018]. Available at: http://www.bordatech.com/.

[9] A. Rasheed, E. Iranmanesh, A. S. Andrenko and K. Wang, "Sensor integrated RFID tags driven by energy scavenger for sustainable wearable electronics applications," 2016 IEEE International Conference on RFID Technology and Applications (RFID-TA), Foshan, 2016, pp. 81-86.

[10] A. Rashee, E. Iranmanes, W. Li, X. Fen, A. S. Andrenk and K. Wan, "Experimental study of human body effect on temperature sensor integrated RFID tag," 2017 IEEE International Conference on RFID Technology & Application (RFID-TA), Warsaw, 2017, pp. 243-247.

[11] D. Patron, W. Mongan, T. P. Kurzweg, A. Fontecchio, G. Dion, E. K. Anday, and K. R. Dandekar, "On the use of knitted antennas and inductively coupled RFID tags for wearable applications," IEEE Transactions on Biomedical Circuits and Systems, vol. 10, no. 6, pp. 1047-1057, 2016.

[12] A. Rebecca. "RFID technologies: supply-chain applications and implementation issues." Information systems management 22.1 (2005): 51-65.

[13] Y. Feng, L. Xie, Q. Chen and L. Zheng, "Low-cost printed chipless RFID humidity sensor tag for intelligent packaging," in IEEE Sensors Journal, vol. 15, no. 6, pp. 3201-3208, June 2015.

[14] P. Bulter, "Smart packaging—Intelligent packaging for food, beverages, pharmaceuticals and household products," Mater. World, vol. 9, no. 3,pp. 11–13, Mar. 2001.

[15] R. A. Potyrailo, N. Nagraj, Z. Tang, F. J. Mondello, C. Surman, and W. Morris, "Battery-free radio frequency identification (RFID) sensors for food quality and safety," Journal of Agricultural and Food Chemistry, vol. 60, no. 35, pp. 8535–8543, Sep. 2012.

[16] T. Unander, J. Sidén, and H.-E. Nilsson, "Designing of RFID-based sensor solution for packaging surveillance applications," IEEE Sensors Journal, vol. 11, no. 11, pp. 3009–3018, Nov. 2011.

[17] T. Leng, X. Huang, K. H. Chang, J. Chen, M. A. Abdalla, and Z. Hu, "Graphene nanoflakes printed flexible meandered-line dipole antenna on paper substrate for low-cost RFID and sensing applications," IEEE Antennas and Wireless Propagation Letters, Vol. 15, pp. 1565-1568, 2016.

[18] Y. Feng, L. Xie, Q. Chen, and L. R. Zheng, "Low-cost printed chipless RFID humidity sensor tag for intelligent packaging," IEEE Sensors Journal, Vol. 15, pp. 3201-3208, 2015.

[19] D. Shuaib, L. Ukkonen, J. Virkki, and S. Merilampi, "The possibilities of embroidered passive UHF RFID textile tags as wearable moisture sensors," in Proceedings of IEEE 5th International Conference on Serious Games and Applications for Health (SeGAH), Perth, WA, Australia, pp. 1-5, 2nd-4th, April, 2017.

[20] S. Merilampi, T. Björninen, L. Ukkonen, P. Ruuskanen, and L. Sydänheimo, "Embedded wireless strain sensors based on printed RFID tag," Sensor Review, Vol. 31, pp. 32-40, 2011.

[21] S. Caizzone, C. Occhiuzzi, and G. Marrocco, "Multi-chip RFID antenna integrating shape-memory alloys for detection of thermal thresholds," IEEE Transactions on Antennas and Propagation., vol. 59, no. 7, pp. 2488–2494, Jul. 2011.

[22] R. Bhattacharyya, C. Di Leo, C. Floerkemeier, S. Sarma, and L. Ananad, "RFID tag antenna based temperature sensing using shape memory polymer actuation," in 2010 IEEE Sensors, Nov. 2010, pp. 2363–2368.

[23] A. A. Babar, S. Manzari, L. Sydanheimo, A. Z. Elsherbeni and L. Ukkonen, "Passive UHF RFID tag for heat sensing applications," in IEEE Transactions on Antennas and Propagation, vol. 60, no. 9, pp. 4056-4064, Sept. 2012.

[24] G. Marrocco, "Pervasive electromagnetics: sensing paradigms by passive RFID technology," IEEE Wireless Communication, vol. 17, no. 6, pp. 10–17, Dec. 2010.

[25] X. Yi, T. Wu, Y. Wang, R. T. Leon, M. M. Tentzeris, and G. Lantz, "Passive wireless smart-skin sensor using RFID-based folded patch antennas," International Journal of Smart and Nano Materials, vol. 2, no. 1, pp. 22–38, Jan. 2011.

[26] B. Cook, A. Shamim, and M. Tentzeris, "Passive low-cost inkjet-printed smart skin sensor for structural health monitoring," IET Microwaves, Antennas & Propagation, vol. 6, no. 14, pp. 1536–1541, Nov. 2012.

[27] T. T. Thai, H. Aubert, P. Pons, M. M. Tentzeris, and R. Plana, "Design of a highly sensitive wireless passive RF strain transducer," in Proceedings of 2011 IEEE MTT-S International Microwave Symposium, Baltimore, MD, USA, pp. 1–4, 5th-10th, June, 2011.

[28] R. A. Potyrailo, and C. Surman, "A passive radio-frequency identification (RFID) gas sensor with self-correction against fluctuations of ambient temperature". Sensors and Actuators B: Chemical, Vol. 185, pp. 587-593, 2013.

[29] L. Yang, R. Zhang, D. Staiculescu, C. Wong, and M. M. Tentzeris, "A novel conformal RFID-enabled module utilizing inkjet-printed antennas and carbon nanotubes for gas-detection applications," IEEE Antennas and Wireless Propagation Letters, vol. 8, pp. 653–656, Jul. 2009.

[30] T. Le, V. Lakafosis, S. Kim, B. Cook, M. M. Tentzeris, Z. Lin, and C. P. Wong, "A novel graphene-based inkjet-printed WISP-enabled wireless gas sensor," in Proceedings of 42nd European Microwave Conference, Amsterdam, Netherlands, pp. 412–415, 29th Octorber-1st November, 2012.

[31] S. Bouaziz, F. Chebila, A. Traille, P. Pons, H. Aubert, and M. M. Tentzeris, "Novel microfluidic structures for wireless passive temperature telemetry medical systems using radar interrogation techniques in Ka-band," IEEE Antennas and Wireless Propagation Letters, vol. 11, pp. 1706–1709, Feb. 2013.

[32] S. T. Qureshi, T. Björninen and J. Virkki, "Referenced backscattering compression level indicator based on passive UHF RFID tags," 2018 IEEE International Conference on RFID Technology & Application (RFID-TA), Macau, 2018, pp. 1-3.

[33] X. Chen, L. Ukkonen and T. Björninen, "Passive E-Textile UHF RFID-based wireless strain sensors with integrated references," in IEEE Sensors

Journal, vol. 16, no. 22, pp. 7835-7836, Nov.15, 2016.

[34] D. Le, Y. Kuang, Leena Ukkonen, T. Björninen, " Microstrip transmission line model fitting approach for characterization of textile materials as dielectrics and conductors for wearable electronics," in International Journal of Numerical Modelling Electronic Networks Devices and Fields, Feb. 2019

[35] Xiang Zhou and Gang Wang, "Study on the influence of curving of tag antennas on performance of RFID system," 2004 Asia-Pacific Radio Science Conference, 2004. Qingdao, China, 2004, pp. 54-57.